Protoplasma (2022) 259:855–867
https://doi.org/10.1007/s00709-021-01704-3

ORIGINAL ARTICLE

Coordination mechanism of cell and cyanelle division in the glaucophyte alga *Cyanophora sudae*

Nobuko Sumiya[1,2]

Received: 29 May 2021 / Accepted: 2 September 2021 / Published online: 23 September 2021

Abstract

In unicellular algae with a single chloroplast, two mechanisms coordinate cell and chloroplast division: the S phase–specific expression of chloroplast division genes and the permission of cell cycle progression from prophase to metaphase by the onset of chloroplast division. This study investigated whether a similar mechanism exists in a unicellular alga with multiple chloroplasts using the glaucophyte alga *Cyanophora sudae*, which contains four chloroplasts (cyanelles). Cells with eight cyanelles appeared after the S phase arrest with a topoisomerase inhibitor camptothecin, suggesting that the mechanism of S phase–specific expression of cyanelle division genes was conserved in this alga. Inhibition of peptidoglycan synthesis by β-lactam antibiotic ampicillin arrested cells in the S–G2 phase, and inhibition of septum invagination with cephalexin resulted in cells with two nuclei and one cyanelle, despite inhibition of cyanelle division. This indicates that even in the unicellular alga with four chloroplasts, the cell cycle progresses to the M phase following the progression of chloroplast division to a certain division stage. These results suggested that *C. sudae* has two mechanisms for coordinating cell and cyanelle division, similar to the unicellular algae with a single chloroplast.

Keywords Cyanelle division · Glaucophyte · Cell cycle · *Cyanophora*

Introduction

Cyanophora is a unicellular glaucophyte alga. In this alga, chloroplasts (also called cyanelles) retain a peptidoglycan layer between the inner and outer envelope membranes (Sato et al. 2009). This characteristic indicates that the cyanelle is in an evolutionary intermediate stage between cyanobacteria and chloroplasts. Further, the cyanelle division system is unique in terms of being in the intermediate stage between cyanobacteria and chloroplasts. Plastids of land plants and algae divide using the plastid-dividing (PD) machinery (Chen et al. 2018). At the division site, electron-dense rings are formed on both the cytosolic and stromal sides of the envelope and are referred to as the outer and inner PD rings (Mita and Kuroiwa 1989). Cyanobacterial-derived FtsZ assembles into a ring as a scaffold of other cyanobacterial-derived PD proteins on the stromal side of the envelope (Osteryoung et al. 1998; Mori et al. 2001). MinD and MinE negatively regulate the FtsZ assembly and assist FtsZ for the formation of a ring at the correct position (Fujiwara et al. 2008). On the cytosolic side of the envelope, the dynamin-related protein DRP5B generates the force for the outer PD ring (Miyagishima et al. 2003; Gao et al. 2003; Yoshida et al. 2006). In contrast to this plant and algal PD system, the cyanelle contains no DRP5B and an outer PD ring (Iino and Hashimoto 2003; Sato et al. 2009; Miyagishima and Kabeya 2010). During a cyanelle division, first, the FtsZ ring and the inner PD ring-like structure are formed on the stromal side of the division site (Iino and Hashimoto 2003; Sato et al. 2009). At the bacterial cell division site, the synthesis of peptidoglycan by FtsI (PBP3) occurs along with the contraction of the FtsZ ring and inner envelope membrane (Spratt and Pardee 1975; Botta and Park 1981; Nanninga 1991). The glaucophyte alga *Cyanophora paradoxa* genome encodes the FtsI homolog, the mRNA of which is increased

Handling Editor: Tsuneyoshi Kuroiwa

✉ Nobuko Sumiya
sumiyan@edu.k.u-tokyo.ac.jp

[1] Department of Biology, Keio University, 4-1-1 Hiyoshi, Kohoku-ku, Yokohama 223-8521, Japan

[2] Present Address: Department of Integrated Biosciences, Graduate School of Frontier Sciences, The University of Tokyo, 5-1-5 Kashiwanoha, Kashiwa, Chiba 277-8562, Japan

during the division (Price et al. 2019). Thereafter, FtsZ ring and inner envelope membrane constriction occur along with septum invagination. This phenomenon is followed by cyanelle outer membrane constriction along with peptidoglycan septum splitting by the hydrolyzing enzyme DipM, which is involved in peptidoglycan hydrolysis at the bacterial division site (Miyagishima et al. 2014). Therefore, the cyanelles divide by a mechanism similar to the bacterial division.

In unicellular algae, which have only a single chloroplast, S phase–specific chloroplast division gene transcription regulates the timing of the onset of chloroplast division (Miyagishima et al. 2012). The chloroplast division machinery, mostly composed of S phase–specific transcribed chloroplast division proteins, divides the chloroplast from the S to the G2 phase. If the onset of chloroplast division is inhibited, cell cycle progression is arrested at prophase. This means that the onset of chloroplast division permits the cell cycle progression from prophase to metaphase (Sumiya et al. 2016). These mechanisms allow the coordination of cell and chloroplast division. Previous studies have been conducted in algae with one or two chloroplasts per cell. It is currently unknown whether the inhibition of chloroplast division results in cell cycle arrest regardless of the number of chloroplasts per cell. In the present study, a glaucophyte alga, *Cyanophora sudae*, which contains four cyanelles, was investigated (Takahashi et al. 2014). By arresting this alga in the S or M phase with inhibitors, I showed that cyanelle division genes are expressed in an S phase–specific manner. Additionally, I demonstrated that the inhibition of peptidoglycan synthesis arrested the cell cycle at the S–G2 phase and that the inhibition of septum invagination allowed cell cycle progression despite the impairment of cyanelle division. These results indicated that the mechanism for coordinating cell and chloroplast division is conserved even in the alga with four chloroplasts.

Materials and methods

Algal culture

Cyanophora sudae strain Takah. & Nozaki NIES-764 was obtained from the algal collection of the National Institute for Environmental Studies (Tsukuba, Japan). The cells were cultured in CSi medium (Kasai et al. 2004) in a 100-mL test tube at 20 °C under continuous light at 80 µmol photons m^{-2} s^{-1} with 1 L/min aeration by ambient air. A hemocytometer was used for counting the number of cells from three independent cultures. For antibiotic treatment, a 1/5,000 volume of 10 mg/mL camptothecin stock solution in methanol, 1/2,500 volume of 10 mg/mL propyzamide stock solution in methanol, 0–3/50,000 volume of 5 mg/mL ampicillin stock solution in distilled water, or a 0–1/500 volume of 1 mg/mL cephalexin stock solution in distilled water was added to the culture, which was precultured without the inhibitor for 3 days.

Transcriptomic survey of orthologous genes of cell and cyanelle division genes

Log-phase cells (5×10^8) were harvested via centrifugation at $500 \times g$ for 5 min and stored at − 140 °C until use. Total RNA was extracted using the Sepasol-RNA I Super G (Nacalai tesque). Thereafter, genomic DNA was eliminated with the RNase-Free DNase Set and RNeasy Mini Kit (Qiagen). The paired-end cDNA library created from 520 µg of total RNA was sequenced using the Illumina HiSeq 4000 system by Eurofins Genomics (Tokyo, Japan). The raw sequence reads were deposited in the DNA Data Bank of Japan (DDBJ) sequence read archive (DRA) with accession no. DRA011817 and experiment no. DRX275855. Sequence quality of reads was assessed using FastQC (Andrews 2010), and reads were trimmed with Trimmomatic (Bolger et al. 2014). The de novo transcriptome assembly was performed using Trinity (Grabherr et al. 2011). BLAST searches on the assembled data were performed by SequenceServer (Priyam et al. 2019) using known sequences from other land plants and algae.

RNA extraction and quantitative RT-PCR

Cells were harvested by centrifugation at $500 \times g$ for 5 min after keeping them undisturbed for 12 h in a 50-mL conical tube at 4 °C; the harvested cells were stored at − 140 °C until use. Cells were broken by vortexing with 0.5-mm-diameter zirconia beads in 1 mL of Sepasol-RNA I super G after incubation for 5 min at room temperature; the homogenate was centrifuged at $12{,}000 \times g$ for 10 min at 4 °C. To the supernatant, 100 µL of 1-bromo-3-chloropropane was added and centrifuged at $12{,}000 \times g$ for 18 min at 4 °C after vortexing. The upper aqueous phase was mixed with an equal volume of EtOH, and total RNA was purified with the RNeasy Mini Kit and RNase-Free DNase set. Quantitative RT-PCR analyses were performed using a StepOnePlus Real-Time PCR system (Thermo Fisher Scientific) and TB Green Premix Ex Taq II (Tli RNaseH Plus) (TaKaRa Bio), according to the manufacturer's instructions. The primer sequences are presented in Table S1. The values of *proliferating cell nuclear antigen* (*PCNA*) (accession no. ICRL01000002), *cyclin B* (accession no. ICRL01000001), *cell division cycle protein 20* (*cdc20*) (accession no. ICRL01000005), *FtsZ* (accession no. ICRL01000003), *minD* (accession no. ICRL01000006), and *DipM* (accession no. ICRL01000004) were normalized with *LSU rRNA* (accession no. ICRL01000007). Serially

diluted solutions were used for generating standard curves. The data was obtained from three independent cultures.

Immunoblot analyses

Cells were harvested by centrifugation at 500 × *g* for 5 min after leaving undisturbed for 12 h in a 50-mL conical tube at 4 °C; the harvested cells were stored at − 140 °C until use. An immunoblot analysis was performed according to the protocol by Sumiya et al. (2016) using the following primary antibodies: anti-β-tubulin (1:2000, T5293, Sigma-Aldrich), anti-H3S10ph (1:2000, Abcam, ab5176), anti–*C. paradoxa* MinD (1:1000, Miyagishima et al. 2012), and anti–*C. paradoxa* FtsZ (1:1000, Miyagishima et al. 2012). A goat anti-rabbit (Bio-Rad, 1706515) or anti-mouse IgG HRP (Bio-Rad, 1706516) antibody was used as a secondary antibody at a dilution of 1:2000.

SYBR Green I staining and immunofluorescence staining

Cells were harvested by centrifugation at 500 × *g* for 5 min after leaving undisturbed for 12 h in a 50-mL conical tube at 4 °C. For SYBR Green I staining, 10 ng/mL SYBR Green I nucleic acid gel stain (Thermo Fisher Scientific, S7585) was used for staining the cells in PBS buffer (0.13 M NaCl, 7 mM Na_2HPO_4, 3 mM NaH_2PO_4, pH 7.2). Three independently cultured cells were stained with SYBR Green I, and the frequencies of the cells in each cell cycle stage were counted. Inhibitor-treated cells with markedly strong cyanelle autofluorescence were judged as dead or heavily damaged cells. Only live cells were used to calculate the frequencies of the cells in each cell cycle stage. For immunofluorescence staining, the anti-H3S10ph (1:200) was used as the primary antibody and goat anti-rabbit IgG conjugated with Alexa Fluor 488 antibody (1:200, Thermo Fisher Scientific, A-11034) was used as the secondary antibody, as described in Sumiya et al. (2016). An epifluorescence microscope (Eclipse 80i, Nikon) equipped with a CCD camera (DS-Fi3-L4, Nikon) was used for the examination of cells. A GFP-B cube was used for acquiring the images of SYBR Green I fluorescence and anti-rabbit IgG conjugated with Alexa Fluor 488 antibody. A B-2A cube was used for acquiring the images of autofluorescence of chlorophyll.

Statistical analysis

All data were obtained using three independently cultured cells and statistically analyzed using Student's *t*-test as described in the figure legends.

Results

Cell cycle of C. sudae

Reportedly, *Cyanophora sudae* retains 2–8 cyanelles and genetically 4 cyanelles (Takahashi et al. 2014). The cell cycle of *C. sudae* was divided into five stages based on cell and cyanelle morphologies (Fig. 1a). Stage I cells contained one nucleus and two kidney-shaped cyanelles. Cyanelle nucleoids were round in shape. In stage II, the cyanelle nucleoids became kidney-shaped, and cyanelles became dumbbell-shaped. Stage III cells contained four cyanelle nucleoids and four cyanelles. In stage IV, the nucleus was transformed into a wedge shape, following which in stage V, nuclear division and cytokinesis occurred. Cells were stained with the M phase marker—the histone H3 at serine 10 (H3S10ph) antibody (Fujiwara et al. 2013)—to combine these morphological stages with the cell cycle stage (Fig. 1b). H3S10ph signals to the nuclei of the cells were observed in stages III, IV, and V. Furthermore, H3S10ph signals were observed in some stage I cells immediately after cytokinesis. These results suggested that the stage III cells were in prophase, stage IV ones were in metaphase, stage V cells with two nuclei and no clear cytoplasmic division plane were in anaphase, and stage V cells undergoing cytokinesis were in telophase (Fig. 1c). However, it cannot be proven that the antibody penetrates the cytosol of all observed cells, so it is difficult to identify that all stage III cells are in prophase.

Effects of cell cycle arrest on cyanelle division

C. sudae cells proliferated with a doubling time of 25.3 ± 3.75 h under continuous light (Fig. 2a). Under this condition, 50–60% of the cells are stage III cells, 20–40% are stage I cells, and ~ 20% are stage II cells. Few stage IV and V cells were observed. No cells with 8 cyanelles were observed in the culture conditions. The cell cycle progression was inhibited using inhibitors to examine whether the cell cycle stage regulates the onset of cyanelle division. When cells were cultured in the presence of 2 µg/mL of the DNA synthesis inhibitor camptothecin, at 48 h after camptothecin addition, cell growth ceased with the number of cells being doubled compared with that at the beginning. At 72 h after camptothecin addition, 83.5% of the cells contained 4 cyanelles. Furthermore, 16% of the cells contained 8 cyanelles, which were not observed in the control (Fig. 2a, b). To examine the changes of mRNA levels of the cell cycle and cyanelle division marker genes, full-length cDNA sequences from exponentially growing cells were obtained by whole transcriptome analysis. The

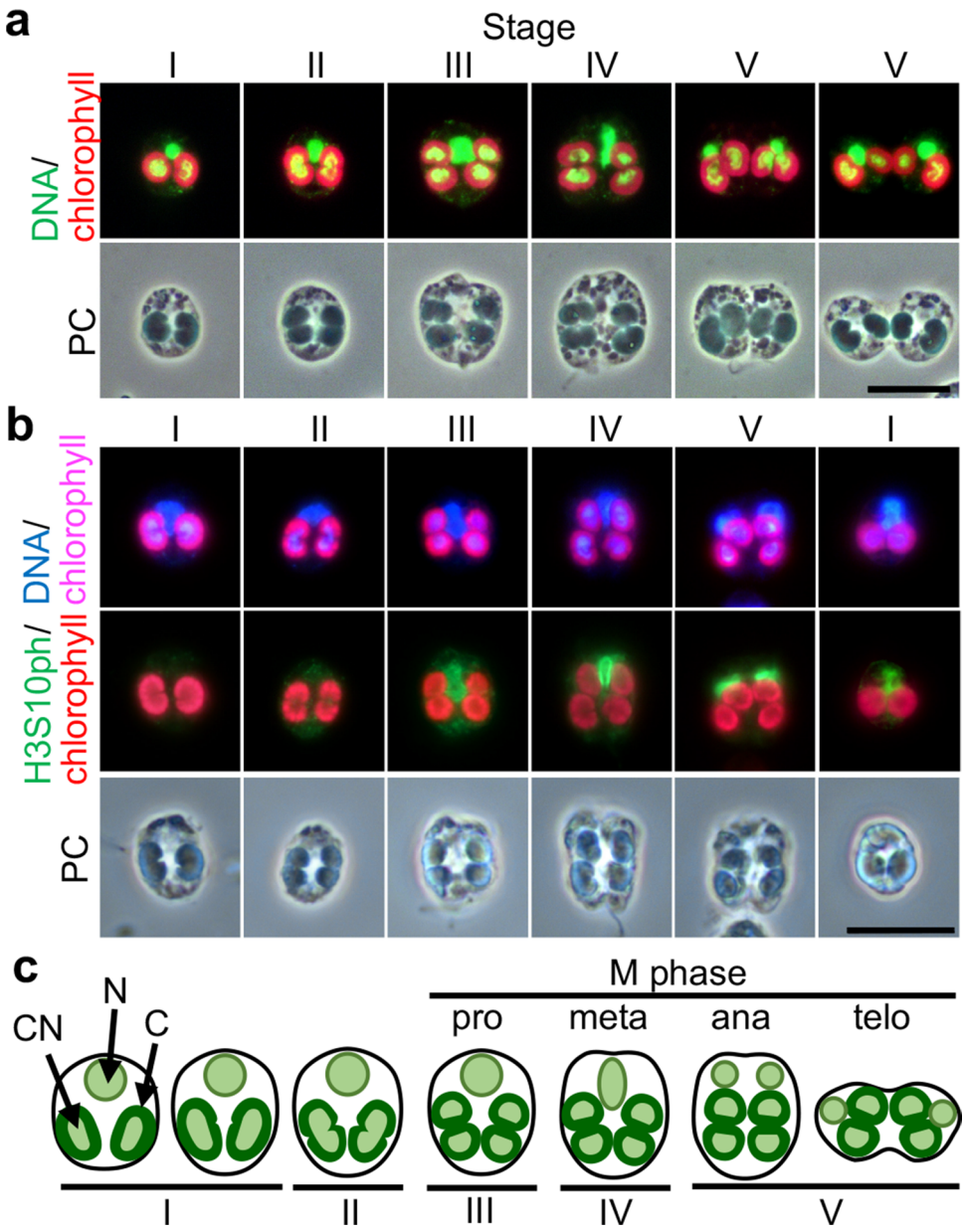

Fig. 1 Cell cycle of *Cyanophora sudae*. **a** SYBR Green I–stained cells demonstrating that cell cycle of *C. sudae* is divided into five stages according to morphological differences. Green displays SYBR Green I–stained DNA. Red displays autofluorescence of chlorophyll. PC is phase contrast. Scale bar = 10 µm. **b** Immunofluorescence images of M phase marker H3S10ph. Blue displays DAPI-stained DNA. Red displays autofluorescence of chlorophyll. Green displays H3S10ph. Scale bar = 10 µm. **c** Schematic diagram of *C. sudae* cell cycle. N indicates the nucleus, C indicates chloroplasts (cyanelles), and CN indicates cyanelle nucleoids

sequences of *proliferating cell nuclear antigen* (*PCNA*, an S phase marker), *cell division cycle protein 20* (*Cdc20*, an M phase marker), *cyclin B* (a G2/M phase marker), *FtsZ*, *DipM*, and *MinD* were obtained by BLAST P search. Multiple sequence alignment was performed with the Clustal W program (Larkin et al. 2007). The results demonstrated that the characteristic domains and motifs of each protein were conserved in these putative sequences (Supplemental Figs. 1–6). Thereafter, primers for real-time PCR analysis were designed, and the mRNA levels of the cell cycle markers in cells cultured for 0, 1.5, and 3 days without the inhibitor were analyzed (Supplemental Fig. 7a). *PCNA* mRNA levels gradually decreased; however, *cdc20* and *cyclin B* mRNA levels did not show significant changes. The decrease in the level of the S phase marker suggested that the cells began entering the stationary state 3 days after the transfer. The mRNA levels of the cyanelle division genes, *FtsZ*, *DipM*, and *MinD*, were examined with the primers designed from the obtained sequences, but there were no significant changes in *FtsZ*, *DipM*, and *MinD* mRNA levels. Then, the mRNA levels of the cell cycle markers in cells cultured for 0, 1.5, and 3 days with 2 µg/mL camptothecin were analyzed (Fig. 2c). *PCNA* mRNA level gradually increased in the presence of camptothecin; however, *cdc20* and *cyclin B* mRNA levels were considerably decreased under the 3-day camptothecin treatment. Changes in the protein levels of the cell cycle and marker proteins were also examined. In cells cultured

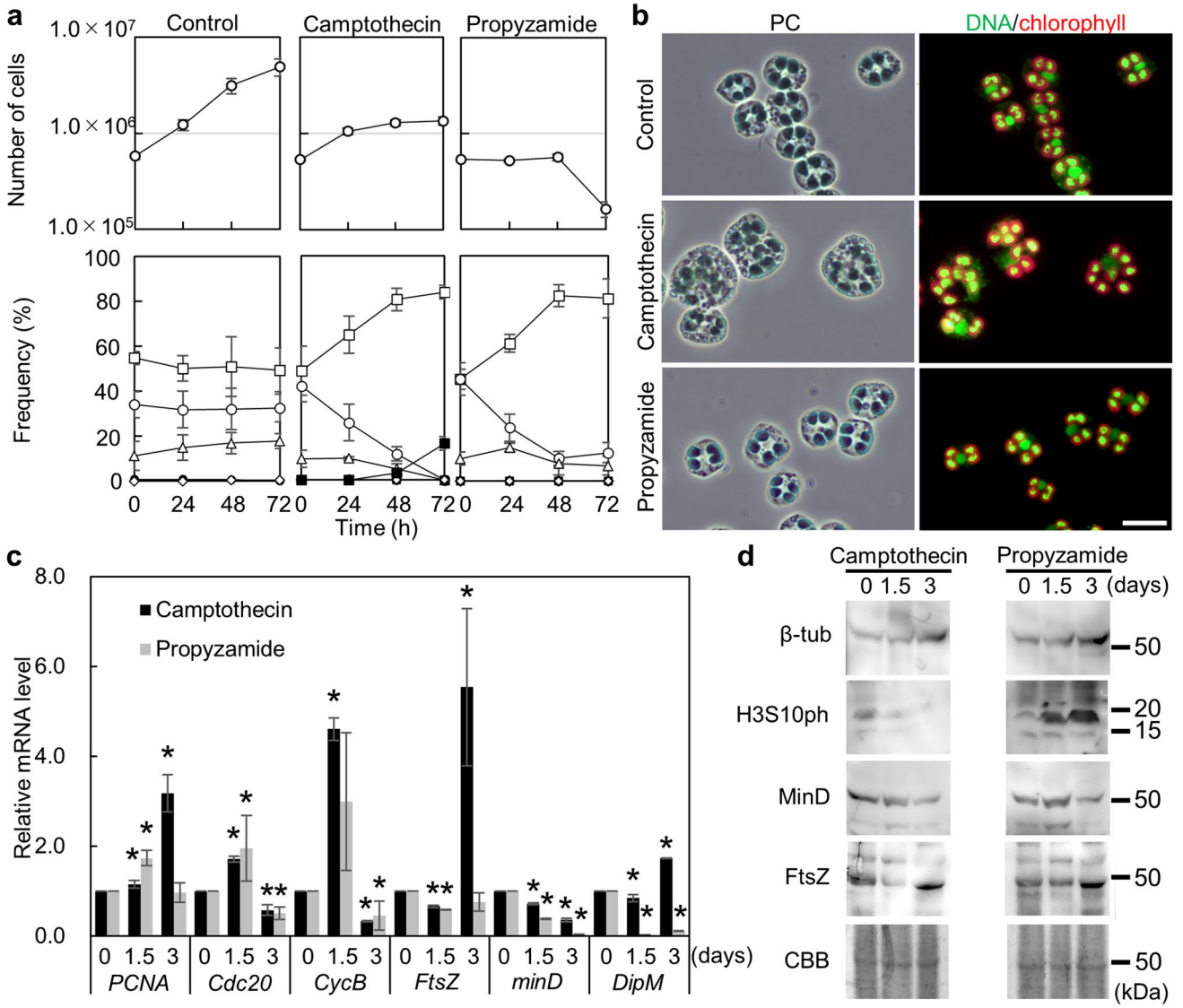

Fig. 2 Effect of S phase or M phase arrest on the progression of cell cycle and cyanelle division cycle. **a** Growth of cells with or without an inhibitor. *C. sudae* cells were cultured under continuous light for 72 h with 0.5 μM methanol (control), 2 μg/mL of DNA synthesis inhibitor camptothecin in methanol, or 0.4 μg/mL propyzamide in methanol. The upper graphs display the changes in the number of cells. The lower graphs display the changes in the frequency of the cells in stages I (opened circles), II (opened triangles), III (opened squares), and IV (opened diamonds). Filled squares display the frequency of the cells with eight cyanelles. The error bars indicate the SD of three independent cultures. **b** Cell images 72 h after the incubation with the inhibitor. PC: phase contrast. Green: SYBR Green I–stained DNA. Red: autofluorescence of chlorophyll. Scale bar = 10 μm. **c** Quantitative RT-PCR analyses demonstrating the transcript levels of cell cycle and cyanelle division marker genes in the cells treated with camptothecin or propyzamide for 0, 1.5, or 3 days. *PCNA* is an S phase marker. *Cyclin B* (*CycB*) is a G2/M phase marker, and *cdc20* is an M phase marker. *FtsZ*, *minD*, and *DipM* are cyanelle division genes. Expression levels in the cells just after transfer were defined as 1.0; *LSU rRNA* was used as the internal control. The error bars indicate the SD of three independent cultures. Asterisks indicate a significant difference against the level at 0 days (Student's *t*-test, $P < 0.05$). **d** Immunoblot analyses demonstrating the protein levels of cell cycle and cyanelle division markers in the 0, 1.5, or 3 days treated with camptothecin or propyzamide cells. β-tubulin is an S/M phase marker. H3S10ph is an M phase marker. *MinD* and *FtsZ* are cyanelle division genes. Coomassie brilliant blue (CBB) staining of the gel is displayed as a loading control

for 0, 1.5, and 3 days without the inhibitor, the S and M phase marker β-tubulin protein was decreased, and the M phase marker H3S10ph did not change (Supplemental Fig. 7b). In the presence of 2 μg/mL camptothecin, β-tubulin was gradually increased, and the M phase marker H3S10ph was decreased (Fig. 2d). These data indicated that cells were arrested at the S phase after 72-h incubation with 2 μg/mL camptothecin as expected. The mRNA levels of the cyanelle division genes were next examined in the presence of camptothecin. The accumulations of *FtsZ* and

DipM mRNA levels were confirmed in S phase–arrested cells using real-time PCR analysis. Conversely, *MinD* mRNA level, which negatively impacts chloroplast division, decreased (Fig. 2c). Immunoblotting with the FtsZ and MinD antibodies of *C. paradoxa* (Miyagishima et al. 2014) revealed that there were no changes in FtsZ and MinD levels during the 3 days of culture without inhibitor (Supplemental Fig. 7b), but there was a decrease in MinD levels and an increase in FtsZ levels in the presence of camptothecin (Fig. 2d). Although the DipM antibody of *C. paradoxa* (Miyagishima et al. 2014) did not detect DipM in *C. sudae* (data not displayed), based on real-time PCR results, it is likely that when the cells were arrested in the S phase in the presence of camptothecin, the genes constituting the cyanelle division apparatus continued to be expressed.

Treatment with 0.4 µg/mL of a microtubule-decomposing drug propyzamide inhibited cell growth at 48 h after propyzamide addition. The number of cells substantially decreased 72 h after the treatment (Fig. 2a) due to cell death. Here, 83.5% of the cells contained 4 cyanelles (Fig. 2a, b). No significant increase was observed in *cdc20* and *cyclin B* mRNA levels after 72-h incubation (Fig. 2c). However, immunoblot analysis demonstrated that β-tubulin and H3S10ph levels were increased (Fig. 2d). The accumulation of H3S10ph level indicated that cells were arrested at the M phase after 72-h incubation with 0.4 µg/mL of propyzamide. In these cells, *minD* and *DipM* mRNA levels were decreased. Furthermore, the decrease in minD protein level was confirmed by immunoblot analysis. Conversely, FtsZ protein was accumulated 72 h after the beginning of treatment (Fig. 2d).

Effects of inhibition of peptidoglycan synthesis on cell cycle progression

The effect of cyanelle division inhibition on cell cycle progression was investigated. Analysis of *C. paradoxa* showed that inhibiting peptidoglycan synthesis by β-lactam antibiotic ampicillin inhibits septum formation and delays constriction (Sato et al. 2007). Therefore, ampicillin treatment of *C. sudae* should inhibit septum formation. First, the appropriate concentrations of ampicillin were examined. Regarding changes in the number of the cells 72 h after ampicillin addition (0–1.5 µg/mL), the results suggested that treatment with > 0.75 µg/mL ampicillin affected cell growth and that with 1.5 µg/mL ampicillin caused the decrease in the number of the cells 48 h after beginning the treatment (Fig. 3a). The ratio of the morphological stages demonstrated that the ratio of stage III cells was transiently decreased but rebounded 72 h after the treatment with 0.5–1.0 µg/mL ampicillin. Since stage III cells were defined as cells with four cyanelles, the increase in the frequency of stage III cells means that the inhibitory effect of ampicillin on cyanelle division lasted only for a short period at concentrations less than 1.0 µg/mL. Conversely, treatment with 1.5 µg/mL ampicillin caused an increase in stage I cells, which contained two cyanelles, and a decrease in stage III cells throughout the treatment (Fig. 3b). Besides the accumulation of stage I cells, cells containing a single cyanelle and nucleus that were not observed in the ampicillin-untreated cells appeared in the ampicillin-treated cells (Fig. 3c). The cells with a single nucleus and cyanelle would have resulted from single cytokinesis of stage I cells under the inhibition of cyanelle division. Therefore, 1.5 µg/mL ampicillin was deemed the most suitable for examining the effect of ampicillin treatment; however, the growth curve showed that some cells were dead during the 1.5 µg/mL ampicillin treatment. In the presence of 1.5 µg/mL ampicillin, the S phase marker *PCNA* mRNA was accumulated (Fig. 4a). *Cdc20* mRNA level was decreased, whereas *cyclin B* mRNA level was slightly increased. Immunoblot results showed that the S/M phase marker β-tubulin remained accumulated, whereas the M phase marker H3S10ph was decreased (Fig. 4b). In this condition, *FtsZ*, *minD*, and *DipM* mRNA levels were drastically decreased (Fig. 4a). Moreover, MinD protein level was decreased but no change was observed in FtsZ protein level during the 3-day treatment period (Fig. 4b). The FtsZ arc or FtsZ ring is formed in the cyanelle of the ampicillin-treated *C. paradoxa* (Sato et al. 2007). Therefore, the FtsZ protein detected in the ampicillin-treated *C. sudae* would be localized as the arc or ring structure.

Effects of septum invagination inhibitor on cell cycle progression

The appropriate concentration of FtsI inhibitor cephalexin was then examined. Compared with ampicillin, which inhibits PBP1a, PBP1b, and FtsI (Curtis et al. 1979), cephalexin only inhibits FtsI (Chung et al. 2009) in *Escherichia coli*. Cephalexin treatment inhibits membrane invagination at division sites (Daley et al. 2016). In *C. sudae*, compared with the control, the cell growth rate decreased with the > 0.2 µg/mL cephalexin treatment (Fig. 5a). The number of cells at 72 h after treatment with > 0.25 µg/mL cephalexin decreased after the cells had increased, suggesting that some cells were dead during the cephalexin treatment. The ratio of the morphological stage of the cells treated with > 0.2 µg/mL cephalexin showed that cephalexin addition decreased the frequency of stage III cells. The frequency of stage I cells and that of the cells with one nucleus and cyanelle were increased. The decrease in the number of stage III cells with four cyanelles and the parallel increase in the number of stage I cells with two cyanelles and those with one nucleus and cyanelle indicated that cephalexin treatment inhibits cyanelle division but allows the cell cycle to progress. Furthermore, the cells with two nuclei and one

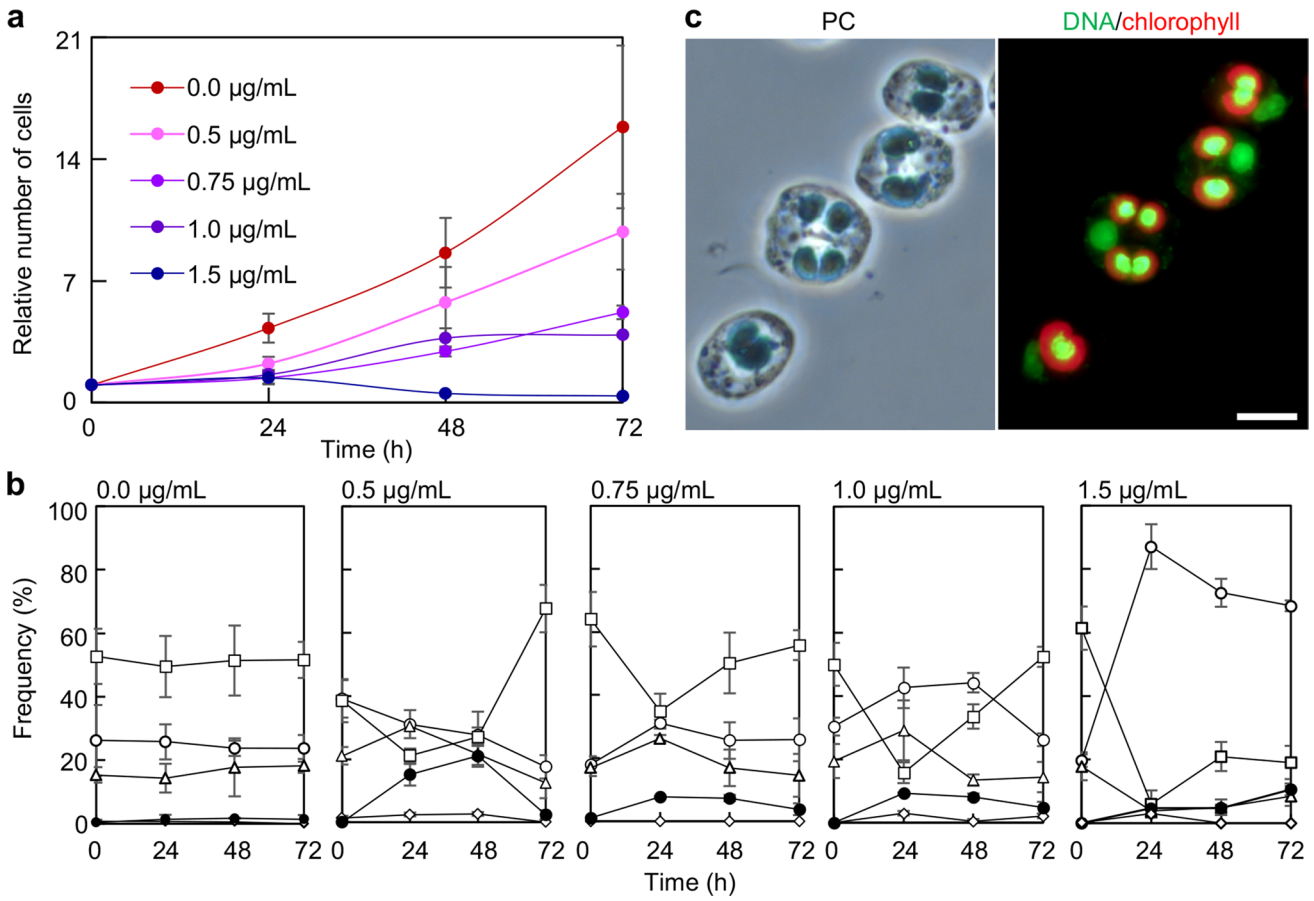

Fig. 3 Effect of ampicillin treatment on the growth of *C. sudae*. **a** Growth curve of *C. sudae* after the addition of different concentrations of ampicillin. The number of the cells just after transfer was defined as 1.0. **b** Changes in the frequency of cells in stages I (opened circles), II (opened triangles), III (opened squares), and IV (opened diamonds). Filled circles display the frequency of cells with one nucleus and one cyanelle. The error bars indicate the SD of three independent cultures. **c** Relative cell images after 72-h treatment with 1.5 µg/mL ampicillin. Green display SYBR Green I–stained DNA. Red displays autofluorescence of chlorophyll. PC is phase contrast. Scale bar = 10 µm

cyanelle were observed after treatment with > 0.4 µg/mL cephalexin (Fig. 5b, c). Among the cephalexin concentrations tested, 2.0 µg/mL displayed the clearest changes in the ratio of the morphological stage. The frequency of stage I cells increased from 28.2% ± 5.5% to 74.8% ± 6.1% during the 24-h cephalexin treatment and then gradually decreased. The frequency of the cells with one nucleus and one cyanelle increased from 1.3% ± 1.1% to 64.7% ± 2.2% during the 48-h cephalexin treatment and that of the cells with two nuclei and one cyanelle increased from 0% ± 0% to 11.1% ± 2.7% during the 72-h cephalexin treatment. Although some cells died, these clear time-course changes in the frequency of the cells in each cell cycle stage suggested that 2.0 µg/mL cephalexin was most suitable for examining the effect of the cephalexin treatment.

In the 2.0 µg/mL cephalexin-treated cells, *PCNA* mRNA was accumulated, whereas *cdc20* and *cyclin B* mRNA levels were decreased (Fig. 6a). In these cells, β-tubulin and H3S10ph levels were increased during the cephalexin treatment (Fig. 6b). The number of nuclei and cyanelles in the cells 72 h after treatment with cephalexin was examined using immunofluorescent staining with the anti-H3S10ph antibody (Fig. 6c). Some cells in the M phase retained one cyanelle and two nuclei, suggesting that the cell cycle progressed but cyanelle division was inhibited at the stage of septum invagination. Taken together, these data suggested that in cephalexin-treated cells, cell cycle progression was inhibited in most cells, potentially at the S phase; however, in some cells, the cell cycle progressed despite cyanelle division being inhibited.

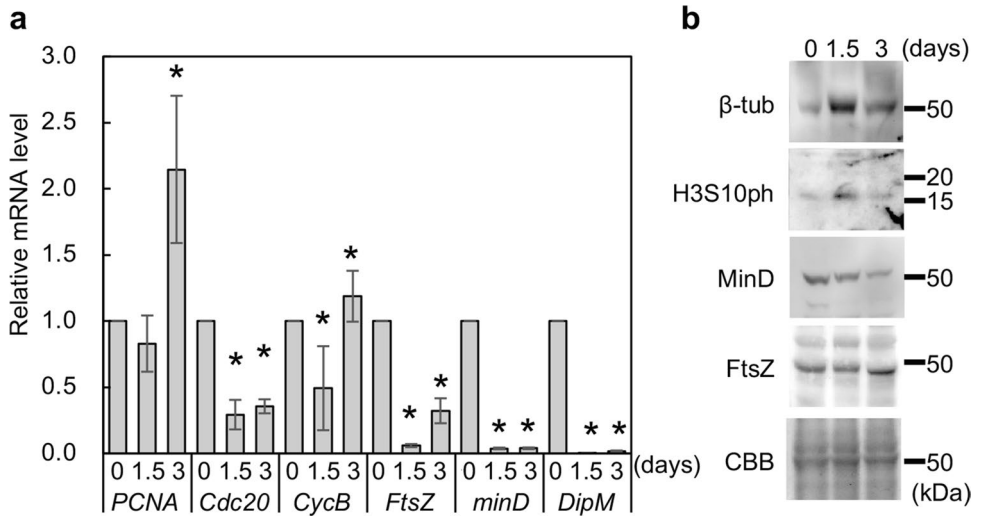

Fig. 4 Effect of ampicillin treatment on the expression of cell and cyanelle division genes. **a** Quantitative RT-PCR analyses demonstrating the transcript levels of cell cycle and cyanelle division marker genes in the cells treated with 1.5 μg/mL ampicillin for 0, 1.5, or 3 days. *PCNA* is an S phase marker. *CycB* is a G2/M phase marker, and *cdc20* is an M phase marker. *FtsZ*, *minD*, and *DipM* are cyanelle division genes. Expression levels in the cells just after transfer were defined as 1.0; *LSU rRNA* was used as the internal control. The error bars indicate the SD of three independent cultures. Asterisks indicate a significant difference against the level at 0 days (Student's *t*-test, $P < 0.05$). **b** Immunoblot analyses displaying the protein levels of cell cycle and chloroplast division markers in the cells treated 0, 1.5, or 3 days with ampicillin. β-tubulin is an S/M phase marker. H3S10ph is an M phase marker. *MinD* and *FtsZ* are cyanelle division genes. CBB staining of the gel is displayed as a loading control

Discussion

S phase–specific transcription of cyanelle division genes

In unicellular algae containing a single chloroplast, the coordination mechanism of cell and chloroplast division is considered to be regulated by two mechanisms: (1) the expression of chloroplast division genes is restricted to the S phase and (2) the cell cycle progresses from the prophase to metaphase following the onset of contraction at the chloroplast division site (Miyagishima et al. 2012; Sumiya et al. 2016; Sumiya 2018). The former has been reported in various algae (Miyagishima et al. 2012). However, the latter has been investigated only in algae containing a single chloroplast. In the present study, I examined whether *C. sudae*, which contains four cyanelles, exhibits these two mechanisms. In S phase–arrested *C. sudae*, the number of cyanelles per cell increased (Fig. 7a); moreover, the expression levels of the cyanelle division genes *FtsZ* and *DipM* were increased, whereas that of *MinD*, which represses the FtsZ ring formation, was decreased. The number of chloroplasts reportedly increased in the unicellular red alga *Cyanidioschyzon merolae* arrested at the S phase, possibly because chloroplast division apparatus is formed specifically during the S phase and continued to be formed under S phase arrest (Itoh et al. 1996; Miyagishima et al. 2012). As with *C. merolae*, the increase in the number of cyanelles per cell in S phase–arrested *C. sudae* cells will be owing to the undegraded cyanelle division apparatus. In the M phase–arrested cells, although the FtsZ protein level was increased, the number of cyanelles per cell was not increased. The increase in the FtsZ protein level contradicts the result that cyanelles did not divide in the M phase–arrested cells. Cyanelles of the propyzamide-treated *C. sudae* cells were not spherical-shaped but were kidney-shaped with a flat division plane. In *C. paradoxa*, the kidney-shaped cyanelles exhibit the FtsZ arc (Sato et al. 2007). Although the present study failed to confirm the FtsZ localization via immunostaining with anti-FtsZ antibodies for the green alga *Nannochloris bacillaris* (Koide et al. 2004) or *Cyanophora paradoxa* (Miyagishima et al. 2012) (data not displayed), FtsZ accumulation in the M phase–arrested *C. sudae* could be derived from the FtsZ arc. Considering that the accumulation of FtsZ protein level in the M phase–arrested *C. sudae* is due to the FtsZ arc, there will be no contradiction between the stopping of cyanelle division in the M phase–arrested cells and the increase in FtsZ protein level. These suggested that the expression of cyanelle division genes is mainly restricted to the S phase, except for minD, which negatively regulates cyanelle division in *C. sudae*. As a result, the formation of the cyanelle division apparatus is restricted to the S phase, and the onset of cyanelle division is confined to the S phase.

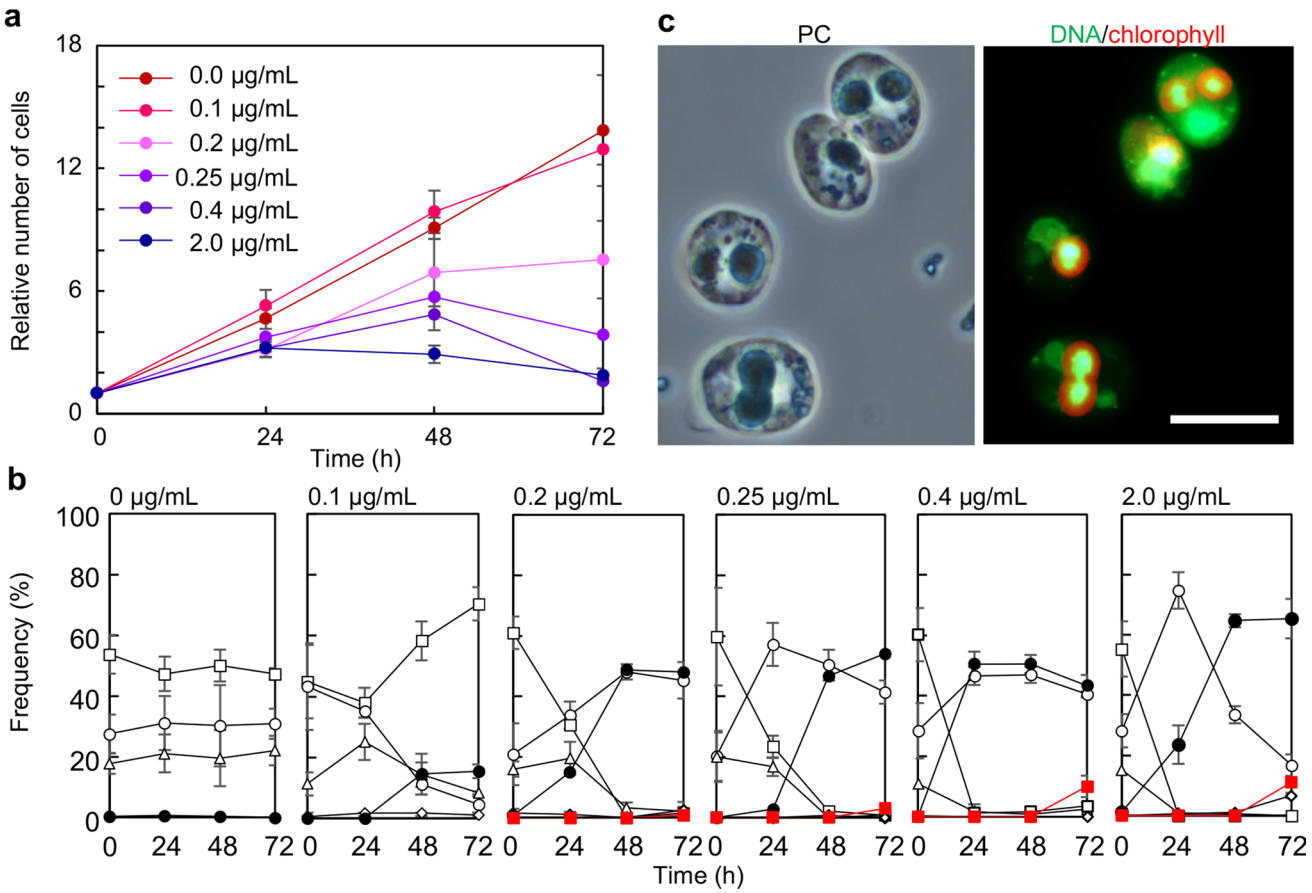

Fig. 5 Effect of cephalexin treatment on the growth of *C. sudae*. **a** The growth curve of *C. sudae* after the addition of different concentrations of cephalexin. **b** The changes in the frequency of cells in stages I (opened circles), II (opened triangles), III (opened squares), and IV (opened diamonds). Filled circles display the frequency of the cells with one nucleus and one cyanelle. Red squares display the frequency of cells with two nuclei and one cyanelle. The error bars indicate the SD of three independent cultures. **c** Relative cell images after 72-h treatment with 2.0 μg/mL cephalexin. Green display SYBR Green I–stained DNA. Red displays autofluorescence of chlorophyll. PC is phase contrast. Scale bar = 10 μm

Cyanelle division arrest inhibits cell cycle progression

Treatment with β-lactam antibiotics inhibits the progression of cyanelle division as well as cell cycle progression in glaucophyte *C. paradoxa*. The cyanelle of the ampicillin-treated *C. paradoxa* contains an FtsZ arc or a ring but inhibits septum formation (Sato et al. 2007). Carbenicillin treatment arrests the cell cycle of *C. paradoxa* at a certain point before the anaphase (Sumiya et al. 2016). In *C. sudae*, stage I cells composed 88% of the total cells 24 h after 1.5 μg/mL ampicillin addition. This phenomenon was attributed to the cells that were in stages II–V at the time of ampicillin addition being divided once and then arrested at a certain stage before the metaphase (Fig. 7b). Because a certain number of cells died during the 1.5 μg/mL ampicillin treatment, the death of stage II–V cells may have increased the proportion of stage I cells. It was difficult to determine whether the cells in stage I were the divided cells during the ampicillin treatment or remained in stage I throughout the treatment. Matsumoto et al. (2012) succeeded in distinguishing cells just after division by the microtubule-depolymerization inhibitor colchicine using the unicellular charophyte *Closterium peracerosum–strigosum–littorale* complex. However, *C. sudae* does not have a rigid cell wall, and it is hard to distinguish the cells just after division, even with the microtubule-organization inhibitor. The presence of 10% of the cells with a single nucleus and cyanelle at 72 h after ampicillin addition, which was not observed in the control, eliminated this possibility. This is because the cells with two cyanelles can only be considered to have arisen through one cell division of stage I cells under the inhibition of cyanelle division. Which stage of the cell cycle do the stage I cells correspond to? Because the cells in stages III–V were in the M phase (Fig. 1c), cells in stages I and II were in the G1, S, or G2 phase. In the present study, the cells with kidney-shaped cyanelles are defined as stage I cells and those with dumbbell-shaped cyanelles as stage II

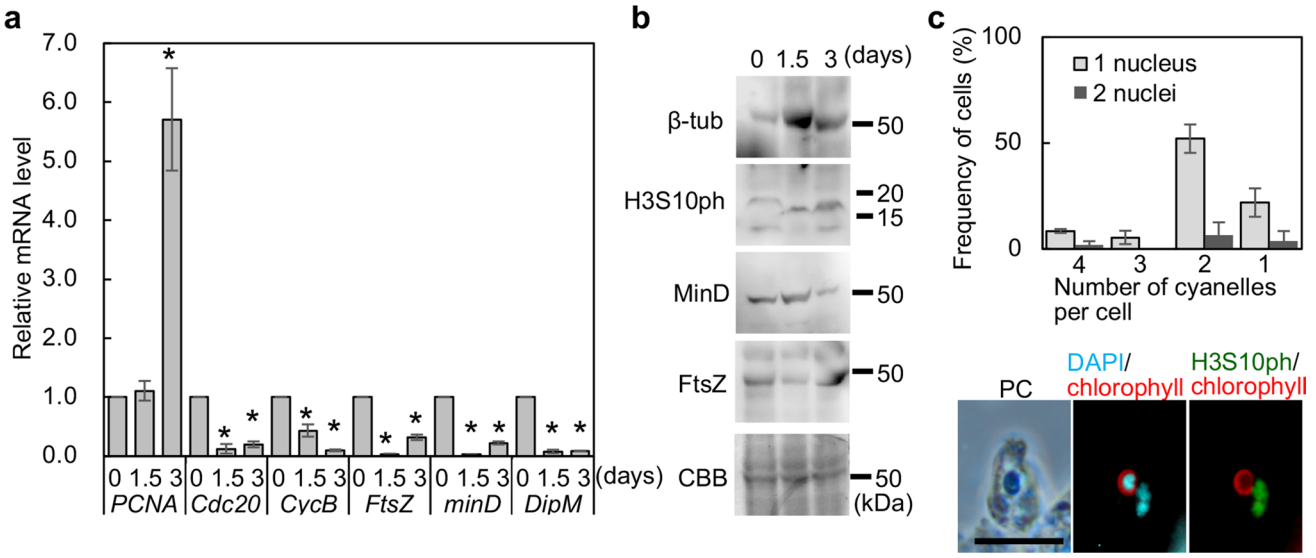

Fig. 6 Effect of cephalexin treatment on expression of cell and cyanelle division genes. **a** Quantitative RT-PCR analyses displaying the transcript levels of cell cycle and cyanelle division markers in the cells treated with 2.0 μg/mL cephalexin for 0, 1.5, or 3 days. *PCNA* is an S phase marker. *CycB* is a G2/M phase marker, and *cdc20* is an M phase marker. *FtsZ*, *minD*, and *DipM* are cyanelle division genes. Expression levels in the cells just after transfer were defined as 1.0; *LSU rRNA* was used as the internal control. The error bars indicate the SD of three independent cultures. Asterisks indicate a significant difference against the level at 0 days (Student's *t*-test, $P < 0.05$). **b** Immunoblot analyses displaying the protein levels of cell cycle and chloroplast division markers in the cells treated 0, 1.5, or 3 days with cephalexin. β-tubulin is an S/M phase marker. H3S10ph is an M phase marker. *MinD* and *FtsZ* are cyanelle division genes. CBB staining of the gel is displayed as a loading control. **c** The number of the cyanelles of the H3S10ph-positive cells in the cells treated with 2.0 μg/mL cephalexin for 3 days. The light gray bar shows the frequency of cells with one nucleus, and the dark gray bar shows the frequency of cells with two nuclei. The error bars indicate the SD of three independent cultures. The lower images display the immunofluorescence images of the cell with two nuclei and one cyanelle. Blue displays DAPI-stained DNA. Red displays autofluorescence of chlorophyll. Green displays H3S10ph. Scale bar = 10 μm

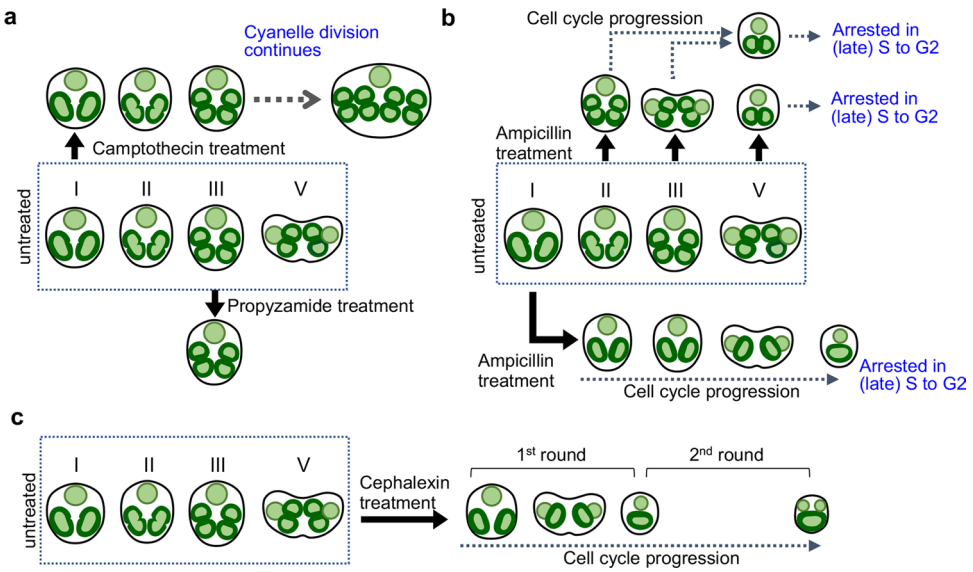

Fig. 7 Schematic diagram of effects of inhibitors. **a** Summary of the results of camptothecin or propyzamide treatment. S phase arrest using camptothecin causes an increase in the number of cyanelles. Propyzamide treatment arrests the cell cycle at the M phase with four cyanelles. **b** Summary of the result of ampicillin treatment. Ampicillin treatment impairs the peptidoglycan synthesis and inhibits cyanelle division at the early stage of cyanelle division. Stage I cells with two cyanelles divide without cyanelle division to become cells with a single cyanelle. Stage II–V cells with four cyanelles divide without cyanelle division to become cells with two cyanelles. Cells are arrested in the S–G2 phase. **c** Summary of the result of cephalexin treatment. Cephalexin treatment impairs the septum invagination and inhibits cyanelle division at the mid-phase of cyanelle division. The cell cycle progresses despite cyanelle division being inhibited. Cells with two nuclei and one cyanelle arise with two rounds of cell division without cyanelle division

cells. The kidney-shaped cyanelles contain the FtsZ arc, and the dumbbell-shaped cyanelles contain the FtsZ ring in *C. paradoxa* (Sato et al. 2007). Based on the results of S phase arrest by camptothecin, the cyanelle division apparatus of *C. sudae* would be formed in the S phase. Therefore, stage I cells should be in the G1–S phase, and stage II cells should be in the S–G2 phase. The completion of cytokinesis in the ampicillin-treated stage I cells suggested that despite the inhibition of cyanelle division early in the S phase, cytokinesis could be completed at least once. No cells with two nuclei were observed after ampicillin treatment; therefore, the inhibition of cyanelle division by β-lactam antibiotics suppressed cell cycle progression at a certain stage prior to metaphase, as observed in *C. paradoxa* (Sumiya et al. 2016). Similar to *C. merolae* and *C. paradoxa*, *C. sudae* would possess a cell cycle checkpoint that confirms the onset of cyanelle division. In ampicillin-treated cells, *PCNA* and *cyclin B* mRNA levels were increased, whereas the *cdc20* mRNA level (an M phase marker) was decreased and H3S10ph was decreased (Fig. 4). Transcription of *cyclin B* reportedly begins at the S phase and peaks at the G2/M phase (Richardson et al. 1992; Bai et al. 1994; Piaggio et al. 1995; Sumiya et al. 2016). Localization of the S phase marker PCNA is detected in the early-S–G2 phase in *C. merolae* (Fujiwara et al. 2013). Therefore, ampicillin-treated cells would be arrested in S–G2 phase. *C. merolae* cells of which chloroplast division is arrested before the onset of the chloroplast division were arrested at prophase and *cyclin B* level in these cells was suppressed (Sumiya et al. 2016). Thus, the mechanism for arresting the cell cycle in the ampicillin-treated *C. sudae* might be different from that in *C. merolae*. In *C. merolae* cells, in addition to the decrease in *cyclin B* level, the migration of cyclin-dependent kinase B (CDKB) during S–G2 phase transition was blocked (Sumiya et al. 2016). Therefore, CDKB might be involved in cell cycle arrest in the ampicillin-treated *C. sudae* cells.

In cephalexin-treated *C. sudae* cells, the percentage of stage I cells increased, followed by an increase in the percentage of cells with a single nucleus and cyanelle; then, the percentage of cells with two nuclei was increased (Fig. 5). Although *cdc20* and *cyclin B* mRNA levels were decreased, *PCNA* mRNA level was increased in the cephalexin-treated cells. Additionally, immunoblot analysis revealed that β-tubulin and H3S10ph levels were increased (Fig. 6). These results indicated that the cell cycle progressed despite the invagination of the peptidoglycan layer being inhibited (Fig. 7c). Ampicillin-treated, peptidoglycan synthesis–inhibited cells were arrested at a certain stage (probably the S–G2 phase), and cephalexin-treated, septum invagination–inhibited cells were not arrested. This indicates that the putative cell cycle checkpoint confirmed the stage before the septum invagination and determined whether to proceed with the cell cycle. Furthermore, the cell cycle of ampicillin-treated cells progressed until the number of cyanelle decreased to one. This indicates that the putative retrograde signal, which communicates the cell cycle regulator, is not lost during the cell cycle progression. The difference between *C. sudae* and other algae with a single chloroplast is that the cell cycle progresses until the number of cyanelle reaches one, even when the onset of cyanelle division is inhibited by peptidoglycan synthesis inhibition. This suggests that *C. sudae*, which retains four cyanelles, does not have a mechanism to strictly recognize and maintain the number of chloroplasts per cell.

In this study, I suggest that *C. sudae*, containing multiple cyanelles, as well as unicellular algae, containing a single chloroplast, would possess two mechanisms for coordinating the cell and cyanelle division cycle. One is the specification of the timing of cyanelle division by the S phase–specific expression of cyanelle division genes, and the other is the permission of cell cycle progression by the onset of cyanelle division. The mutual constraints of cell and cyanelles, which are the determination of the onset of the cyanelle division by the cell and permission of cell cycle progression by the cyanelles, coordinate cell and cyanelle division. These mechanisms are thought to have been acquired during the establishment of chloroplasts and lost during the evolution of land plants. In the pteridophyte *Selaginella nipponica* Fr. et Sav. and the moss *Physcomitrella patens*, ampicillin treatment has no effect on cell cycle progression (Izumi et al. 2003; Katayama et al. 2003). This means that land plants do not have a mechanism for coordinating cell and chloroplast division. In the unicellular charophyte *Closterium peracerosum–strigosum–littorale* complex, which has two chloroplasts, ampicillin treatment inhibits chloroplast division and generates a cell with a single chloroplast (Matsumoto et al. 2012). The division of a cell with a single chloroplast is inhibited, but the nuclear division proceeds. Therefore, the mechanism to coordinate cell and chloroplast division differs in charophytes from rhodophyte *C. merolae* and glaucophytes *C. paradoxa* and *C. sudae*. Further studies in various algae will be needed to understand the evolution of the mechanisms for coordinating cell and chloroplast division in the algae.

Supplementary Information The online version contains supplementary material available at https://doi.org/10.1007/s00709-021-01704-3.

Acknowledgements I thank Dr. Yoshinobu Hayashi (Keio University) for his technical advice and support for RNA-seq analysis and Dr. Shin-ya Miyagishima (National Institute of Genetics) for anti-*Cyanophora paradoxa* FtsZ, minD, and DipM antibodies. Computations were partially performed on the NIG supercomputer at ROIS National Institute of Genetics.

Funding This work was supported by JSPS KAKENHI Grant Number 17K18091, Basic Science Research Projects from The Sumitomo Foundation Grand Number 200251, Keio University Academic

Development Funds for individual Research, and the Research and Education Center for Natural Sciences, Keio University.

Availability of data and material The transcriptome dataset used during the current study was deposited in the DNA Data Bank of Japan (DDBJ) sequence read archive (DRA) with accession no. DRA011817, with experiment no. DRX275855. Other data supporting the findings of this study are available within the article.

Code availability Not applicable.

Declarations

Ethics approval Yes.

Consent to participate Yes.

Consent for publication Yes.

Conflict of interest The author declares no competing interests.

References

Andrews S (2010) FastQC: a quality control tool for high throughput sequence data. Babraham Bioinformatics, Babraham Institute, Cambridge, United Kingdom

Bai C, Richman R, Elledge SJ (1994) Human cyclin F. EMBO J 13:6087–6098

Bolger AM, Lohse M, Usadel B (2014) Trimmomatic: a flexible trimmer for Illumina sequence data. Bioinformatics 30:2114–2120. https://doi.org/10.1093/bioinformatics/btu170

Botta GA, Park JT (1981) Evidence for involvement of penicillin-binding protein 3 in murein synthesis during septation but not during cell elongation. J Bacteriol 145:333–340. https://doi.org/10.1128/JB.145.1.333-340.1981

Chen C, MacCready JS, Ducat DC, Osteryoung KW (2018) The molecular machinery of chloroplast division. Plant Physiol 176:138–151. https://doi.org/10.1104/pp.17.01272

Chung HS, Yao Z, Goehring NW, Kishony R, Beckwith J, Kahne D (2009) Rapid β-lactam-induced lysis requires successful assembly of the cell division machinery. Proc Natl Acad Sci U S A 106:21872–21877. https://doi.org/10.1073/pnas.0911674106

Curtis NA, Orr D, Ross GW, Boulton MG (1979) Affinities of penicillins and cephalosporins for the penicillin-binding proteins of *Escherichia coli* K-12 and their antibacterial activity. Antimicrob Agents Chemother 16(5):533–539. https://doi.org/10.1128/AAC.16.5.533

Daley D, Skoglund U, Söderström B (2016) FtsZ does not initiate membrane constriction at the onset of division. Sci Rep 6:33138. https://doi.org/10.1038/srep33138

Fujiwara MT, Hashimoto H, Kazama Y et al (2008) The assembly of the FtsZ ring at the mid-chloroplast division site depends on a balance between the activities of AtMinE1 and ARC11/AtMinD1. Plant Cell Physiol 49:345–361. https://doi.org/10.1093/pcp/pcn012

Fujiwara T, Tanaka K, Kuroiwa T, Hirano T (2013) Spatiotemporal dynamics of condensins I and II: evolutionary insights from the primitive red alga *Cyanidioschyzon merolae*. Mol Biol Cell 24:2515–2527. https://doi.org/10.1091/mbc.E13-04-0208

Gao H, Kadirjan-Kalbach D, Froehlich JE, Osteryoung KW (2003) ARC5, a cytosolic dynamin-like protein from plants, is part of the chloroplast division machinery. Proc Natl Acad Sci U S A 100:4328–4333. https://doi.org/10.1073/pnas.0530206100

Grabherr MG, Haas BJ, Yassour M et al (2011) Full-length transcriptome assembly from RNA-Seq data without a reference genome. Nat Biotechnol 29:644–652. https://doi.org/10.1038/nbt.1883

Iino M, Hashimoto H (2003) Intermediate features of cyanelle division of *Cyanophora paradoxa* (Glaucocystophyta) between cyanobacterial and plastid division. J Phycol 39:561–569. https://doi.org/10.1046/j.1529-8817.2003.02132.x

Itoh R, Takahashi H, Toda K et al (1996) Aphidicolin uncouples the chloroplast division cycle from the mitotic cycle in the unicellular red alga *Cyanidioschyzon merolae*. Eur J Cell Biol 71:303–310

Izumi Y, Ono K, Takano H (2003) Inhibition of plastid division by ampicillin in the Pteridophyte *Selaginella nipponica* Fr. et Sav. Plant Cell Physiol 44:183–189. https://doi.org/10.1093/pcp/pcg028

Kasai F, Kawachi M, Erata M, Watanabe MM (2004) NIES collection List of Strains. 7th ed., National Institute for Environmental Studies, Tsukuba, Japan

Katayama N, Takano H, Sugiyama M et al (2003) Effects of antibiotics that inhibit the bacterial peptidoglycan synthesis pathway on moss chloroplast division. Plant Cell Physiol 44:776–781. https://doi.org/10.1093/pcp/pcg096

Koide T, Yamazaki T, Yamamoto M et al (2004) Molecular divergence and characterization of two chloroplast division genes, *FtsZ1* and *FtsZ2*, in the unicellular green alga *Nannochloris bacillaris* (Chlorophyta). J Phycol 40:546–556. https://doi.org/10.1111/j.1529-8817.2004.03105.x

Larkin MA, Blackshields G, Brown NP et al (2007) Clustal W and Clustal X version 2.0. Bioinformatics 23:2947–2948. https://doi.org/10.1093/bioinformatics/btm404

Matsumoto H, Takechi K, Sato H et al (2012) Treatment with antibiotics that interfere with Peptidoglycan biosynthesis inhibits chloroplast division in the desmid *Closterium*. PLoS ONE 7:e40734. https://doi.org/10.1371/journal.pone.0040734

Mita T, Kuroiwa T (1989) Division of plastids by a plastid-dividing ring in *Cyanidium caldarium*. In: Tazawa M (ed) Cell dynamics: cytoplasmic streaming cell movement—contraction and migration cell and organelle division phototaxis of cell and cell organelle. Springer Vienna, Vienna, pp 133–152

Miyagishima SY, Kabeya Y (2010) Chloroplast division: squeezing the photosynthetic captive. Curr Opin Microbiol 13:738–746. https://doi.org/10.1016/j.mib.2010.10.004

Miyagishima SY, Nishida K, Mori T et al (2003) A plant-specific dynamin-related protein forms a ring at the chloroplast division site. Plant Cell 15:655–665. https://doi.org/10.1105/tpc.009373

Miyagishima SY, Suzuki K, Okazaki K, Kabeya Y (2012) Expression of the nucleus-encoded chloroplast division genes and proteins regulated by the algal cell cycle. Mol Biol Evol 29:2957–2970. https://doi.org/10.1093/molbev/mss102

Miyagishima SY, Kabeya Y, Sugita C et al (2014) DipM is required for peptidoglycan hydrolysis during chloroplast division. BMC Plant Biol 14:57. https://doi.org/10.1186/1471-2229-14-57

Mori T, Kuroiwa H, Takahara M et al (2001) Visualization of an FtsZ ring in chloroplasts of *Lilium longiflorum* leaves. Plant Cell Physiol 42:555–559. https://doi.org/10.1093/pcp/pce095

Nanninga N (1991) Cell division and peptidoglycan assembly in *Eschenchia coli*. Mol Microbiol 5:791–795. https://doi.org/10.1111/j.1365-2958.1991.tb00751.x

Osteryoung KW, Stokes KD, Rutherford SM et al (1998) Chloroplast division in higher plants requires members of two functionally divergent gene families with homology to bacterial *ftsZ*. Plant Cell 10:1991–2004. https://doi.org/10.1105/tpc.10.12.1991

Piaggio G, Farina A, Perrotti D et al (1995) Structure and growth-dependent regulation of the human cyclin B1 promoter. Exp Cell Res 216:396–402. https://doi.org/10.1006/excr.1995.1050

Price DC, Goodenough UW, Roth R et al (2019) Analysis of an improved *Cyanophora paradoxa* genome assembly. DNA Res 26:287–299. https://doi.org/10.1093/dnares/dsz009

Priyam A, Woodcroft BJ, Rai V et al (2019) Sequenceserver: a modern graphical user interface for custom BLAST databases. Mol Biol Evol 36:2922–2924. https://doi.org/10.1093/molbev/msz185

Richardson H, Lew DJ, Henze M et al (1992) Cyclin-B homologs in *Saccharomyces cerevisiae* function in S phase and in G2. Genes Dev 6:2021–2034. https://doi.org/10.1101/gad.6.11.2021

Sato M, Nishikawa T, Kajitani H, Kawano S (2007) Conserved relationship between FtsZ and peptidoglycan in the cyanelles of *Cyanophora paradoxa* similar to that in bacterial cell division. Planta 227:177–187. https://doi.org/10.1007/s00425-007-0605-0

Sato M, Mogi Y, Nishikawa T et al (2009) The dynamic surface of dividing cyanelles and ultrastructure of the region directly below the surface in *Cyanophora paradoxa*. Planta 229:781–791. https://doi.org/10.1007/s00425-008-0872-4

Spratt BG, Pardee AB (1975) Penicillin-binding proteins and cell shape in *E. coli*. Nature 254:516–517. https://doi.org/10.1038/254516a0

Sumiya N (2018) Mechanism of coordination between cell and chloroplast division in unicellular algae. Plant Morphol 30:83–89. https://doi.org/10.5685/plmorphol.30.83

Sumiya N, Fujiwara T, Era A, Miyagishima SY (2016) Chloroplast division checkpoint in eukaryotic algae. Proc Natl Acad Sci U S A 113:E7629–E7638. https://doi.org/10.1073/pnas.1612872113

Takahashi T, Sato M, Toyooka K et al (2014) Five *Cyanophora* (Cyanophorales, Glaucophyta) species delineated based on morphological and molecular data. J Phycol 50:1058–1069. https://doi.org/10.1111/jpy.12236

Yoshida Y, Kuroiwa H, Misumi O, Nishida K, Yagisawa F, Fujiwara T, Nanamiya H, Kawamura F, Kuroiwa T (2006) Isolated chloroplast division machinery can actively constrict after stretching. Science 313:1435–1438. https://doi.org/10.1126/science.1129689